

Comparison of SEM and Optical Analysis of DT Neutron Tracks in CR-39 Detectors

P.A. Mosier-Boss^{*a}, L.P.G. Forsley^b, P. Carbonelle^c, M.S. Morey^d, J.R. Tinsley^d, J. P. Hurley^d,
F.E. Gordon^a

^aSPAWAR Systems Center Pacific, Code 71730, San Diego, CA, USA 92152;

^bJ JWK International Corp., Annandale, VA 22003 USA;

^cUniversité catholique de Louvain, B-1348 Louvain-la-Neuve, Belgium;

^dNational Security Technologies, LLC, Special Technologies Laboratory, Santa Barbara, CA, USA
93111

ABSTRACT

CR-39 detectors were exposed to DT neutrons generated by a Thermo Fisher model A290 neutron generator. Afterwards, the etched tracks were examined both optically and by scanning electron microscopy (SEM). The purpose of the analysis was to compare the two techniques and to determine whether additional information on track geometry could be obtained by SEM analysis. The use of these techniques to examine triple tracks, diagnostic of 9.6 MeV neutrons, observed in CR-39 used in Pd/D co-deposition experiments will also be discussed.

Keywords: Neutrons, SEM, optical microscopy, SSNTD, triple tracks

1. INTRODUCTION

Columbia Resin 39 (CR-39), a polyallyldiglycol carbonate polymer, has been used as a solid state nuclear track detector (SSNTD) to detect energetic, charged nuclear particles.¹ As an energetic, charged particle traverses through CR-39, it creates along its path an ionization trail that is more sensitive to chemical etching than the bulk material. After etching, the tracks due to energetic particles have the appearance of holes or pits. The size and shape of these pits provides information about the mass, charge, energy, and direction of motion of the particles. The most common method employed to analyze these tracks is optical microscopy. However, atomic force microscopy (AFM)^{2,3} and scanning electron microscopy (SEM)^{4,5} have also been used by others to analyze tracks in CR-39 resulting from exposure to either alpha or proton sources.

CR-39 has also been used to detect neutrons. In order to detect neutrons with CR-39, the neutron must either scatter or undergo a nuclear reaction with the atomic constituents that make up the detector.⁶ The DT neutrons can scatter elastically to create recoil protons, carbons and/or oxygen nuclei in the forward direction. The DT neutrons can also undergo inelastic (n,p) and (n, α) reactions with carbon and oxygen nuclei to create charged particles on both the front and back sides of the CR-39 detector. These knock-on tracks resulting from these interactions will appear uniformly throughout the CR-39 detector. DT neutrons can also undergo the carbon break-up reaction. In this reaction, a metastable ¹³C is formed that then shatters into three alpha particles and a neutron. In the CR-39 detector, the reaction products appear as a triple track in which each prong is caused by an energetic alpha particle. Of the neutron interactions with CR-39, the carbon shattering reaction, resulting in a triple track, is the most easily identifiable. In this communication the use of optical microscopy and SEM to analyze DT-generated tracks, including triple tracks, are compared.

In addition, both optical microscopy and SEM were used to analyze triple tracks that have been observed in CR-39 detectors used in Pd/D co-deposition experiments. The advantage of using CR-39 in these experiments is that CR-39 is

* pam.boss@navy.mil; phone 1 619 553-1603

an example of a constantly integrating detector. Once an event occurs, it is permanently stamped in the plastic. This is particularly useful for events that occur either sporadically or at a low rate. The main disadvantage is that it is not known when those events occurred. The results of the analyses of detectors used in the Pd/D co-deposition experiments are also discussed in this communication.

2. RESULTS AND DISCUSSION

2.1 Neutron Detection Using CR-39 Detectors

Phillips et al.⁷ irradiated CR-39 detectors with neutrons with energies ranging from 0.114 to 14.8 MeV. Figure 1a shows the track size distributions obtained for 0.114, 0.25, 0.565, 1.2, and 14.8 MeV neutrons. It was shown that the track sizes can be used to differentiate recoil protons, recoil carbons/oxygens, and the carbon break-up reaction. The peak at $\sim 10 \mu\text{m}$ is attributed to recoil protons. As the neutron energy increases, the recoil proton peak broadens. At a neutron energy of 1.2 MeV, a second peak is visible at $\sim 25 \mu\text{m}$. This peak is due to recoil carbon and oxygen atoms. For neutron energies between 1.2 and 8 MeV, the size distribution of the tracks are approximately the same. A peak at $\sim 35 \mu\text{m}$ is observed in the size distribution of CR-39 detectors exposed to 14.8 MeV neutrons. This peak is assigned to the carbon break-up reaction that results in triple tracks. Figure 1b shows an optical image of DT-neutron generated tracks. This optical image shows examples of tracks created by recoil protons, carbons, and oxygens as well as the carbon break up reaction.

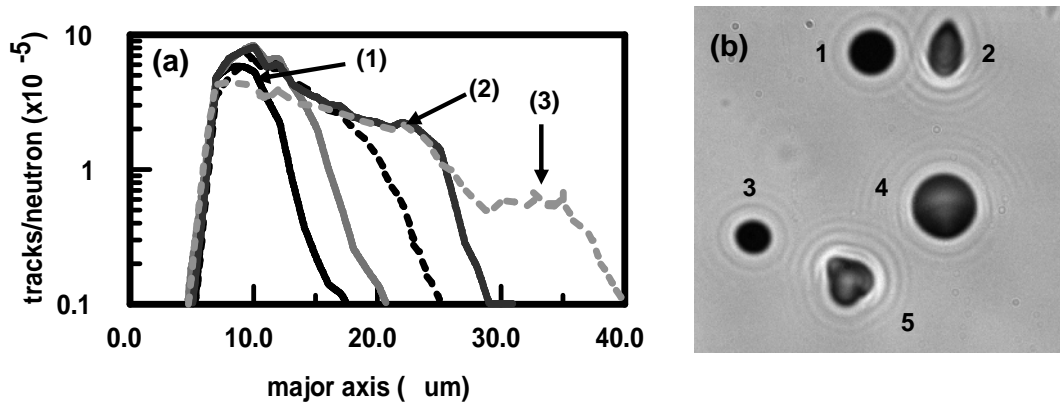


Figure 1. (a) Track size distribution for CR-39 detectors that have been exposed to, from left to right, 0.114, 0.25, 0.565, 1.2, and 14.8 MeV neutrons where (1) indicates the peak due to recoil protons, (2) the peak due to recoil carbon/oxygen atoms, and (3) the peak attributed to the carbon break-up reaction.⁷ (b) DT-neutron generated tracks in CR-39 obtained at 1000x magnification where track #3 is due to a recoil proton; tracks #1, 2, and 4 are due to carbon/oxygen recoils; and track #5 is a triple track created by the carbon break-up reaction.

In the method developed by Phillips et al.,⁷ neutrons with energies between 1.2 and 8.0 MeV cause proton recoils inside the CR-39 detector that exhibit the same track size distribution. Consequently the track size, after a single etch, cannot be used to definitively determine the energy that caused the proton recoil. Fortunately, Roussetski et al.⁸ have developed a sequential etching method that removes this ambiguity. However, this method can only be applied to analyzing proton tracks that are normal incidence to the detector. Figure 2a shows a calibration curve obtained from proton bombardment on CR-39 detectors that had been etched for 7 h at 70°C. Figure 2b shows the track diameter of tracks due to 1.0-2.5 MeV, normal incidence protons as a function of etching time. As shown in Figure 2b, the track size of recoils proton tracks overlap after a single 7 h etch. With increased etching time, the track diameters for the different energy protons increases. However, as shown in Figure 2b, the tracks from the different energy protons do not etch at the same rate. Track etch rate varies inversely with track energy, i.e., the lower the proton energy, the faster the track etches. With

longer etching times, the track sizes spread out making it possible to more accurately determine the energy of the neutron that caused the recoil proton.

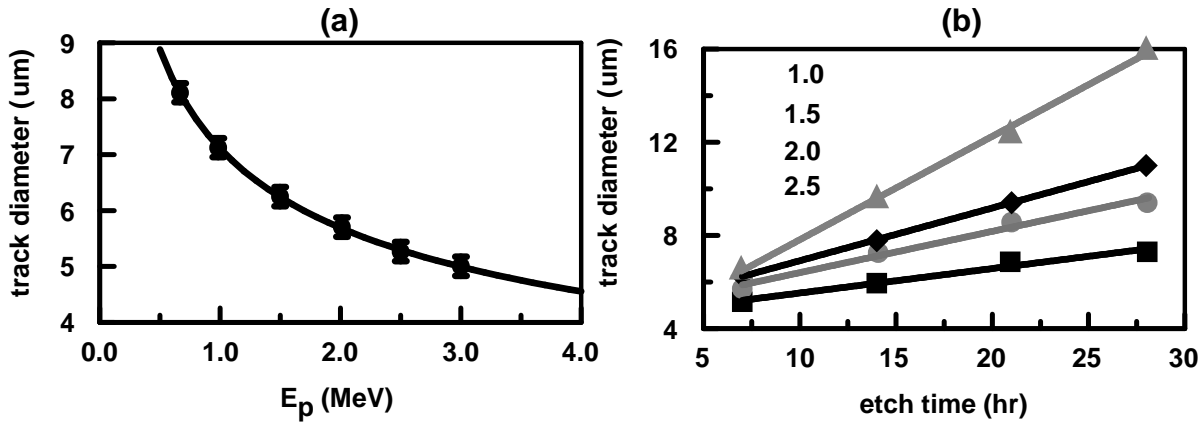


Figure 2.8 (a) Van de Graaf accelerator calibration curve generated for 0.65-3.0 MeV protons of normal incidence with respect to the detector surface. (b) Plot of track diameter vs. etching time for protons of normal incidence for proton energies ranging between 1.0 and 2.5 MeV.

2.2 Analysis of DT neutron Recoil Proton, Carbon, or Oxygen Tracks

Optical and SEM microphotographs of tracks due to a DT neutron proton recoil reaction and a carbon/oxygen recoil reaction are shown in Figures 3a and 3b, respectively. Because the optical images were taken with the detector being backlit, the appearance of the observed image depends upon the manner in which the track has scattered and reflected the light passing through it. Major factors affecting the track appearance are the total internal reflection and inclination angles of elements in a track wall with respect to the light rays.⁹ When the microscope optics are focused on the surface of the detector, the tracks are dark in color, as shown in Figures 1b, 3a(i) and 3b(i). In contrast, the optical images shown in Figures 3a(ii) and 3b(ii) were obtained by overlaying two images – one obtained by focusing the microscope optics on the surface of the detector and the other by focusing on the bottom of the tracks. By overlaying these images and taking into account scattering of light by the pit created by the recoiling proton/oxygen/carbon atom, it is possible to make some conclusions about the three-dimensional shape of the track. In Figure 3a(ii), a bright circle is seen at the bottom of the track. Bright areas inside a track indicate that the light rays coming from below the track are refracted through very small angles in the central area.⁹ As a result, the intensity loss is relatively small causing the central areas to be very bright. Bright features inside a track are indicative of spherical or rounded bottoms. Therefore the bright area inside the track shown in Figure 3a(ii) suggests that the bottom of this track is shallow and rounded. This is confirmed by the SEM image of the track shown in Figure 3a(iii).

In SEM, the sample surface is scanned with a beam of electrons in a raster scan pattern. The signals derived from the electron-sample interactions provide information about the sample including external morphology (texture) and orientation of materials making up the sample. Besides being able to obtain higher resolution images, SEM images have a three dimensional appearance while optical images are inherently two-dimensional. The SEM image of the proton recoil track, Figure 3a(iii) shows that the bottom of the track is rounded. It should be noted that post-SEM, optical analysis of the track did show that electron irradiation did damage the track. Consequently, all optical analysis of the CR-39 detectors needs to be completed prior to SEM analysis.

In contrast to the track shown in Figure 3a(ii), the track shown in Figure 3b(ii) is completely dark. No bright center is observed. Dark areas in the track indicate that total reflection of light has occurred. This is indicative of either steep track walls or a perfectly conical track.⁹ This conclusion is supported by the SEM image of the track shown in Figure 3b(iii). The SEM image shows that the track has steep walls and that the bottom is not rounded.

The results shown in Figure 3 show that optical microscopy and SEM are complimentary techniques to deduce the three dimensional shape of tracks resulting from energetic particle emissions.

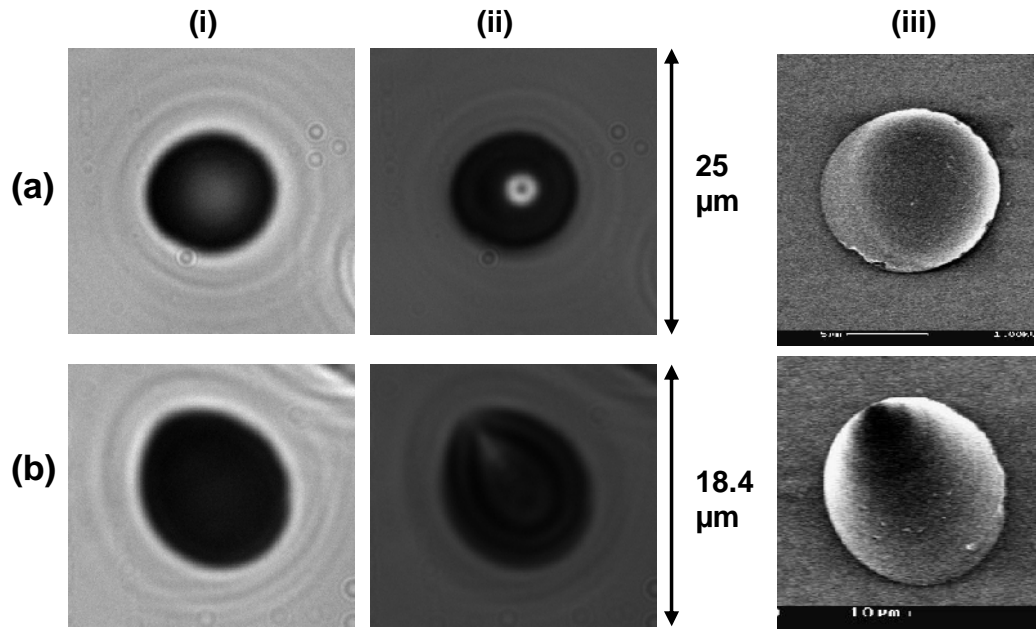
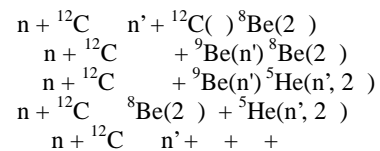


Figure 3. DT-neutron generated tracks in CR-39 where (a) is due to a proton recoil reaction and (b) to either a carbon/oxygen recoil reaction. Both (i) and (ii) are optical images obtained at 1000x magnification where (i) was obtained with the microscope optics focused on the surface of the detector and (ii) obtained by overlaying two images obtained at the surface of the detector and the bottom of the pits. SEM images of the tracks are shown in (iii) where images a(iii) and b(iii) were obtained at magnifications of 5000x and 3000x, respectively.

2.3 Analysis of DT-Neutron Generated Triple Tracks

The carbon breakup reaction can proceed to the four-body final state through one or more of the following reaction mechanisms:¹⁰



The observed relative size and shapes of the lobes comprising the triple track reflect these different processes and can result in both symmetric and asymmetric triple tracks. Examples of both kinds of tracks are discussed *vide supra*. Figure 4 shows optical and SEM micrographs of a symmetric DT-neutron generated triple track. The optical micrographs were taken at a magnification of 1000X. Figure 4a was taken with the microscope optics focused on the surface of the detector while Figure 4b is an overlay of two images taken at the surface and the bottom of the pits. As discussed *vide supra*, the appearance of the observed image depends upon the manner in which the track has scattered and reflected the light passing through it. Again the major factors affecting the track appearance are the total internal reflection and inclination angles of elements in a track wall with respect to the light rays.⁹ Taking these factors into account, and using both the surface and overlay images, Figures 4a and 4b respectively, the 3-dimensional geometry of the triple track can be

deduced. This geometry is important to ascertain the angle of each alpha track relative to the surface of the detector in order to accurately determine the path length, and hence the energy, of each breakup alpha. This angle can not be deduced by simple optical observation alone.

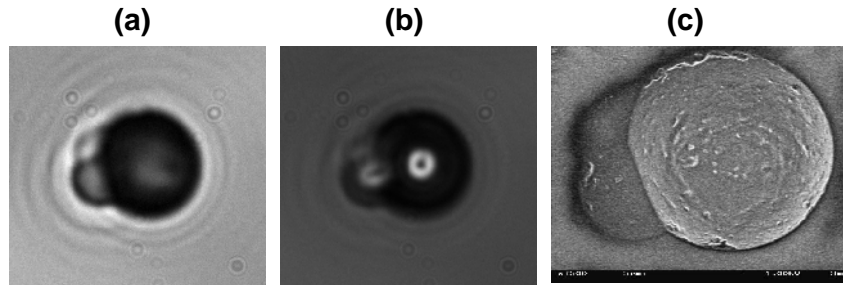


Figure 4. Microphotographs of a symmetric DT-neutron generated triple track. Optical images taken at 1000 x magnification where (a) was obtained with the microscope optics focused on the surface of the CR-39 detector and (b) is an overlay of two images taken at the surface of the detector and the bottom of the pits. (c) A SEM image taken at 7500x magnification.

In the optical photomicrograph shown in Figure 4a, the large center pit is dark in color and the two smaller, left hand tracks are light in color. This suggests that the light colored tracks are shallower than the larger dark one. The optical photomicrograph, Figure 4b, shows bright areas inside the tracks. Bright features inside a track are indicative of spherical or rounded bottoms while dark areas indicate either steep track walls or a perfectly conical track. Comparing the two optical images for the triple track shown in Figure 4, it is concluded that the three alpha tracks comprising the triple track have rounded bottoms and that the two smaller, left hand tracks are shallower than the larger center track. These conclusions are verified by the SEM image of the triple track shown in Figure 4c. The SEM image of the symmetric triple track shows that the bottoms of the three lobes of the triple track are rounded and that the larger track is deeper than the two smaller ones.

Optical and SEM images of an asymmetric triple track are shown in Figures 5a and 5b respectively. In the optical image, Figure 5a, a square indicates the asymmetric triple track. The track is circular in shape with a prong. Next to the triple track is a smaller, brighter circular track. The SEM image, Figure 5b, shows that this small, circular track is shallower than the circular portion of the asymmetric triple track. The prong of the asymmetric triple track observed in the optical image, Figure 5a, is not seen in the SEM image, Figure 5b. This indicates that the prong is actually below the surface of the plastic detector. In the SEM image, the opening of the prong is indicated by an arrow. This undercutting of a track inside the plastic demonstrates that the rate of etching of the ionization trail created by the charged particle in the detector is faster than the etching rate of the bulk material. The results summarized in Figure 5 show that the two methods of analysis can be complementary for tracks caused by the ejection of particles below the surface of the etched detector. The SEM analysis shows which tracks are below the surface of the etched detector and the optical image will show the shape of that track.

2.4 The Pd-D Co-Deposition Process

In the Pd-D co-deposition process an anode and a cathode are immersed in a solution palladium chloride and lithium chloride in deuterated water.¹¹ Palladium is then electrochemically reduced onto the surface of the cathode in the presence of evolving deuterium gas. Electrodes prepared by Pd/D co-deposition exhibit highly expanded surfaces consisting of small spherical nodules. Because of this high surface area and electroplating in the presence of deuterium gas, the incubation time to achieve high D/Pd loadings necessary to initiate low energy nuclear reactions (LENR) is orders of magnitude less than required for bulk electrodes. Besides heat,^{12,13} the following nuclear emanations have been detected using Pd/D co-deposition over a twenty year period of research: X-ray emission,¹⁴ tritium production,¹⁵

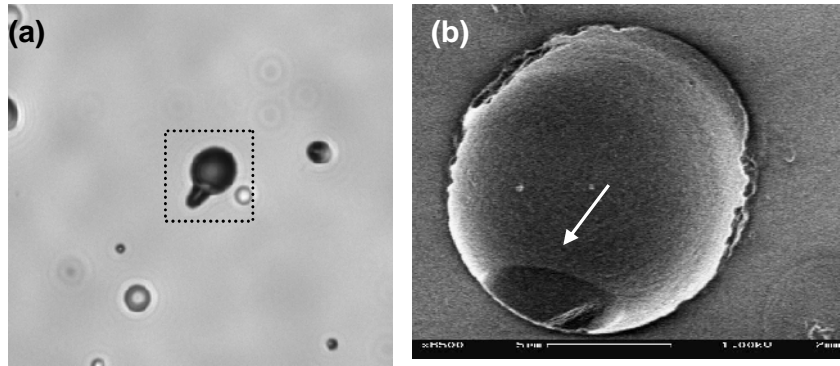


Figure 5. Microphotographs of an asymmetric DT-neutron generated asymmetric triple track. (a) Optical image taken at 200x magnification. (b) SEM image of the region indicated by a square in Figure 2a taken at 6500x magnification. An arrow indicates the opening of the prong seen in the optical image.

transmutation,¹⁶ and charged particle emission.^{17,18} Using the sequential etching method described *vide supra*,⁸ Lipson et al.¹⁹ reported on the observation of DD neutrons in CR-39 detectors used in Pd/D co-deposition experiments.

2.5 Analysis of Pd-D Co-Deposition Generated Triple Tracks

Tracks, observed in CR-39 detectors used in Pd-D co-deposition experiments, coincide with the Pd deposit.¹⁷ A series of control experiments showed that the tracks were not due to radioactive contamination of the cell components nor were they due to either chemical or mechanical damage.¹⁷ Tracks were observed on both the front and back surfaces of the 1 mm thick detectors used in these experiments. In addition to solitary tracks, a small number of symmetric and asymmetric triple tracks have been observed in CR-39 detectors used in Pd-D co-deposition experiments.^{20,21} For an experiment typically running for two weeks, the total number of observed triple tracks on the CR-39 detector, front and back, ranged between 5 and 10 tracks. Triple tracks have not been observed in CR-39 detectors used in control experiments. The time duration of these control experiments was the same as that used in the Pd/D co-deposition experiments. These control experiments indicate that the triple tracks are not the result of cosmic ray spallation neutrons.

Figure 6a shows optical images of a symmetric triple track observed in a Pd/D co-deposition experiment. Optical images of a DT neutron-generated triple track are shown in Figure 6b. The Pd/D generated and the DT-neutron generated triple tracks are indistinguishable. It should be noted that the DT neutron track shown in Figure 6b has a different shape than the triple tracks shown in Figures 1b, 4a and b, and Figure 5a. This supports the notion that the observed relative size and shapes of the lobes comprising the triple track reflect the different reaction mechanisms for the carbon break-up reaction discussed *vide infra*.

In both Figures 6a and 6b, the top images were taken with the microscope optics focused on the surface of the detector and the bottom images are an overlay of two images taken with the optics on the surface and the bottom of the pits. The large lobes of both triple tracks show a bright streak in the center, bottom images of Figures 6a and 4b. This indicates that this lobe is shallow and rounded. The SEM image of the Pd/D co-deposition triple track, Figure 6c, supports this conclusion.

Besides the large lobe, the Pd/D co-deposition generated triple track has two smaller lobes on the left-hand side, Figure 6a. The bottom overlay image shows no bright centers or streaks in the two smaller lobes of this triple track. This suggests that there are either steep track walls or that the track has a conical shape. As shown in the SEM image, Figure 6c, one of the smaller lobes has a conical shape. These results provide further evidence that optical and SEM imaging of tracks complement one another.

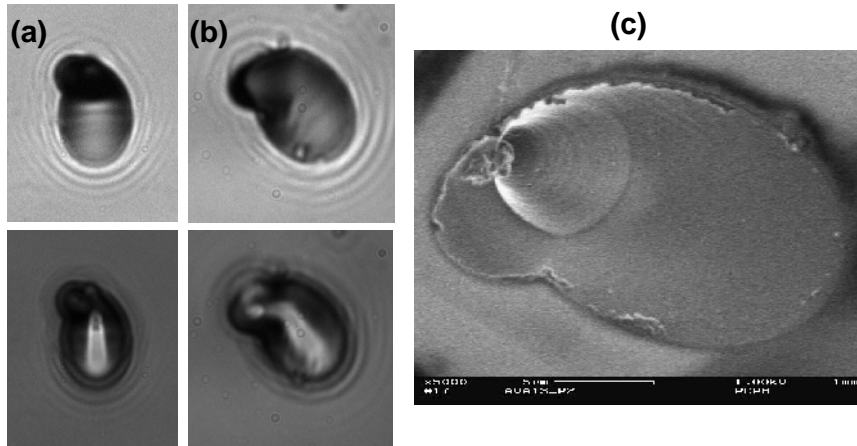


Figure 6. (a) Optical microphotographs of a Pd/D co-deposition generated triple track obtained at 1000x magnification. (b) Optical microphotographs of a symmetric DT-neutron generated triple track obtained at 1000x magnification. In (a) and (b) the top images were taken by focusing the microscope optics on the surface of the CR-39 detector and the bottom images are overlays of two images taken at the surface of the detector and the bottom of the pits. (c) An SEM image of the same Pd/D co-deposition generated triple track shown in (a) taken at 5000x magnification.

3. CONCLUSIONS

In this communication, triple tracks in CR-39 detectors were analyzed by both optical microscopy and SEM. It was shown that the two methods of analyses complimented one another. It was also shown that Pd-D co-deposition generated triple tracks were indistinguishable from DT-neutron generated triple tracks.

4. ACKNOWLEDGEMENTS

This effort was funded by SPAWAR Systems Center Pacific S&T Initiatives Program, the Defense Threat Reduction Agency (DTRA), and JWK Corporation. This manuscript has been authorized by National Security Technologies, LLC, under Contract No. DE-AC52-06-NA25946 with the U.S. Department of Energy. The United States Government retains and the publisher, by accepting the article for publication, acknowledges that the United States Government retains a non-exclusive, paid-up, irrevocable, worldwide license to publish or reproduce the published form of this manuscript, or allow others to do so, for United States Government purposes.

REFERENCES

- [1] Cartwright, B.G., Shirk, E.K., and Price, P.B., "A nuclear-track-recording polymer of unique sensitivity and resolution," *Nucl. Instr. and Meth.*, 153(2-3), 457-460 (1978).
- [2] Palmino, F., Klein, D. and Babrone, J.C., "Observation of nuclear track in organic material by atomic force microscopy in real time during etching," *Rad. Meas.*, 31 (6), 209-212 (1999).
- [3] Yamauchi, T., Mineyama, D., Nakai, H., Oda, K., and Yasuda, N., "Track core size estimation in CR-39 track detector using atomic force microscopy and UV-visible spectrometer," *Nucl. Instr. and Meth. In Phys. Res. B*, 208 (8), 149-154 (2003).

- [4] Oganessian, V.R., Trofimov, V.V., Gaillard, S., Fromm, M., Danziger, M., Hermsdorf, D., and Orelovitch, O.L., "Investigation of the response of thin CR-39 polymer foils irradiated with light ions," Nucl. Instrum. and Meth. In Phys. Res. B, 236 (1-4), 289-294 (2005).
- [5] Rana, M.A., Khan, E.U., Shahzad, M.I., Manzoor, S., Sher, G., and Qureshi, I.E., "Characteristics of antiproton tracks in CR-39," Rad. Meas., 42 (2), 125-129 (2007).
- [6] Frenje, J.A., Li, C.K., Séguin, F.H., Hicks, D.G., Kurebayashi, S., Petrasso, R.D., Roberts, S., Yu Glebov, V., Meyerhofer, D.D., Sangster, T.C., Sources, J.M., Stoeckl, C., Schmid, G.J., and Lerche, R.A., "Absolute measurements of neutron yields from DD and DT implosions at the OMEGA laser facility using CR-39 track detectors," Rev. Sci. Instrum., 73(7), 2597-2605 (2002).
- [7] Phillips, G.W., Spann, J.E., Bogard, J.S., Vo-Dinh, T., Emfietzoglou, D., Devine, R.T., and Moscovitch, M., "Neutron spectrometry using CR-39 track etch detectors," Radiat. Prot. Dosim., 120 (1-4), 457-460 (1996).
- [8] Roussetski, A.S., Lipson, A.G., Lyakhov, B.F., and Saunin, E.I., "Correct identification of energetic alpha and proton tracks in experiments on CR-39 charged particle detection during hydrogen desorption from Pd/PdO:Hx heterostructure," Proceedings of ICCF12, 304-313 (2005).
- [9] Nikezic, D., Yu, K.N., "Formation and growth of tracks in nuclear track materials," Materials Sci. and Eng. R 46(4), 51-123 (2004).
- [10] Antolkovi, B., Dolenc, Z., "The neutron-induced $^{12}\text{C}(n,n')^3$ reaction at 14.4 MeV in a kinematically complete experiment," Nucl. Phys. A 237(2), 235-252 (1975).
- [11] Mosier-Boss, P.A., Dea, J.Y., Gordon, F.E., Forsley, L.P.G., and Miles, M.H., "Review of twenty years of LENR research using Pd/D co-deposition," J. Condensed Matter Nucl. Sci., 4, 173-187 (2011).
- [12] Miles, M.H. and Fleischmann, M., "Measurements of excess power effects in Pd/D₂O systems using a new isoperibolic calorimeter," J. Condensed Matter Nucl. Sci., 4, 45-55 (2011).
- [13] Letts, D., "Codeposition methods: a search for enabling factors," J. Condensed Matter Nucl. Sci., 4, 81-92 (2011).
- [14] Szpak, S., Mosier-Boss, P.A., and Smith, J.J., "On the behavior of cathodically polarized Pd/D system: search for emanating radiation," Phys. Lett. A, 210 (6), 382-390 (1996).
- [15] Szpak, S., Mosier-Boss, P.A., Boss, R.D., and Smith, J.J., "On the behavior of the Pd/D system: evidence for tritium production," Fus. Technol., 33 (1), 38-51 (1998).
- [16] Szpak, S., Mosier-Boss, P.A., Young, C., and Gordon, F.E., "Evidence of nuclear reactions in the Pd lattice," Naturwissenschaften, 92 (8), 394-397 (2005).
- [17] Mosier-Boss, P.A., Szpak, S., Gordon, F.E., and Forsley, L.P.G., "Use of CR-39 in Pd/D codeposition experiments," Eur. Phys. J. Appl. Phys 40 (3), 293-303 (2007).
- [18] Mosier-Boss, P.A., Szpak, S., Gordon, F.E., and Forsley, L.P.G., "Characterization of tracks in CR-39 detectors as a result of Pd/D co-deposition," Eur. Phys. J. Appl. Phys 46 (3), 30901-p1-12 (2009).
- [19] Lipson, A.G., Roussetski, A.S., Saunin, E.I., Tanzella, F., Earle, B., and McKubre, M., "Analysis of the CR-39 detectors from SRI's SPAWAR/Galileo type electrolysis experiment #7 and #5: signature of possible neutron emission," Proceedings of the 8th International Workshop on Anomalies in Hydrogen/Deuterium Loaded Materials, 182-203 (2007).
- [20] Mosier-Boss, P.A., Szpak, S., Gordon, F.E., and Forsley, L.P.G., "Triple tracks in CR-39 as the result of Pd-D co-deposition: evidence of energetic neutrons," 96 (1), 135-142 (2009).
- [21] Mosier-Boss, P.A., Dea, J.Y., Forsley, L.P.G., Morey, M.S., Tinsley, J.R., Hurley, J.P., and Gordon, F.E., "Comparison of Pd/D co-deposition and DT neutron generated triple tracks observed in CR-39 detectors," Eur. Phys. J. Appl. Phys. 51 (2), 20901-p1-p10 (2010).